THE APPLICATION OF IMAGING SPECTROSCOPY DATA IN AGRICULTURE AND HYDROLOGY THE EISAC-89-CAMPAIGN IN THE FREIBURG TEST SITE

H. Bach, W. Mauser

Institute for Physical Geography, Dept. of Hydrology, University of Freiburg, Germany.
Tel.: 0049-761-203-4451, Fax:0049-761-203-4464

Abstract

During the first European Imaging Spectroscopy Campaign 1989, data was acquired of a test-area in the Upper Rhine Valley near the city of Freiburg/Germany using the GER- sensor. An intensive ground truth campaign, conducting an agricultural inventory of all the fields in the 24 km^2 test-area together with filed spectroscopy measurements of selected surfaces was carried out in coincidence with the overflight. This led to digital maps of several vegetation parameters. After the GER-data was radiometrically corrected using the ground- measured reflectance spectra of reference-targets and LOWTRAN-7 modelling of the nadir and off-nadir radiances, geometric registration to the digital maps was carried out. Results of the analysis of the measured airborne spectra of different agricultural surfaces are presented. Data compression was carried out through parameterizing the reflectance edge between 670 nm and 850 nm using an inverted Gaussian model for each pixel in the test-area. The first results show that enhanced information on important agricultural and hydrologic parameters such as changes in the water status from non- irrigated to irrigated fields, degree of plant-coverage and vegetation height can be derived using the available spectral information of this new kind of sensor.

1. THE EISAC'89 CAMPAIGN IN THE FREIBURG TEST- SITE

In May and June 1989 the first European Imaging Spectroscopy Campaign (EISAC) was conducted by JRC and ESA together with additional European research institutes. As one agricultural test-site an area in the Upper Rhine Valley, between the River Rhine and the City of Freiburg (Germany), was selected. The Freiburg test-site contains both agricultural and forested areas. The agricultural area is intensively cultivated, with the main crops being corn (maize), wheat, barley and soybeans. The average field size of app. 1.5 ha is representative for small-scale European farming. Of this test-site data of the GER-sensor, of the FLI (Fluorescence Line Imager) and of a Metric Camera was acquired on June 13, 1989.

2. THE GER-SCANNER DATA

The GER-sensor is an imaging spectroscopy scanner with 63 spectral bands reaching from about 470 nm to 2440 nm. These separate spectrometers enable the measurements in this wide wavelength interval. The documented band-width is 12.5 nm in the visible and 16 nm in the NIR. Table 1 shows the technical specifications of the GER-Scanner.

First analysis of the scanner data shows that band 28 totally failed. The noise in the GER-data is rather high and varies with the spectral region. Band 1 to 6, 32 to 36 and 57 to 63 are very noisy due to detector sensitivity, atmospheric effects and the low amount of radiance at 2.4µm. The signal to noise has been determined to be 5-10 for low reflectance targets at 500 to 600 nm and 20-50 for high reflectance targets at 750 to 850 nm (Richter 1990). Fig. 1 shows an GER-image of band 16, 26 and 48 (red, NIR, MIR) of the test-area near Freiburg. Vegetated areas show up in green, partly covered soils in pink and villages in dark pink. The River Rhine, that shows up rather dark like the

TABLE 1

TECHNICAL SPECIFICATION OF THE GER-SCANNER

- Wavelength Region : 477 nm - 2443 nm
- Numbers of Bands : 63
- 3 Spectrometers:

Wavel. Region	Detector	# Bands	spectral Resolution
477 - 847 nm	Si	31	12.5 nm
1440 - 1800 nm	Pb-S	4	120 nm
2005 - 2443 nm	Pb-S	28	16 nm

- Radiometric Resolution : 16 bit
- IFOV : 3.3 mrad
- GIFOV at 3000 m a. g. : app. 10 m
- Scan-Angle : 90°
- Numbers of Pixels per Scan : 512

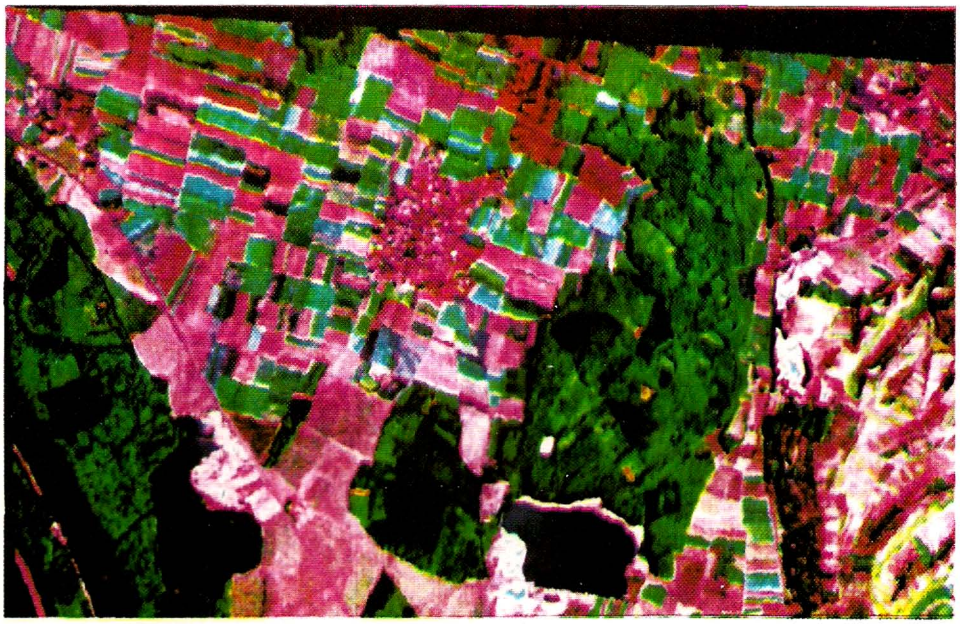

Fig. 1. GER-scanner image; blue = 663 nm, green = 786 nm, red = 2200 nm.

gravel-pit lakes, can be seen in the lower left corner. Great differentiations can be found in the forests with the dark-green to black areas being conifers.

For the processing of the GER-data and ground truth data a PC-based Imaging-Spectroscopy- Workstation was set up. The workstation is equipped with a 512 x 512 x 32 bit display unit. The software supports different data- types (8-, 16-, 32-bit) and a maximum of 64 channels. As an extension of the usual image processing capabilities (Mauser 1988) the software allows to extract spectra of single pixels or arbitrary windows of the imaging spectroscopy data and to combine airborne and field spectroscopic data.

3. GROUND TRUTH

Between June 13 and June 17, 1989 an extensive ground data collection was carried out in an area in the centre of the flight strip. This test-area with an extension of 4*6 km^2 was mapped on the basis of six German Base Maps (1:5000). For each of the 1320 visited fields the following main agricultural features were determined:

1) vegetation type,
2) vegetation height,
3) row distance,
4) degree of soil coverage,
5) plant damages.

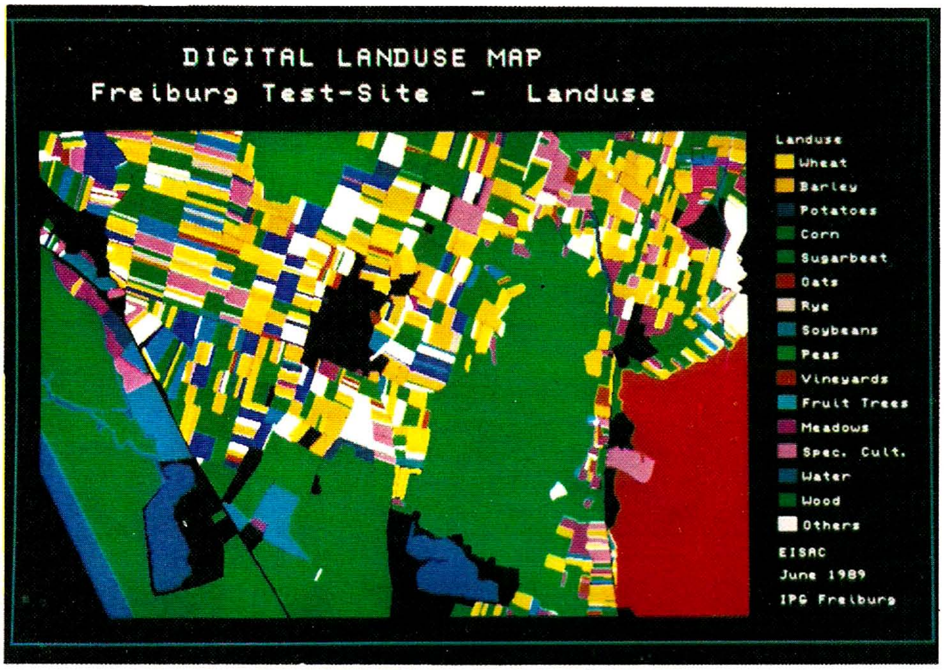

Fig. 2. Digital map of the landuse in the test-area

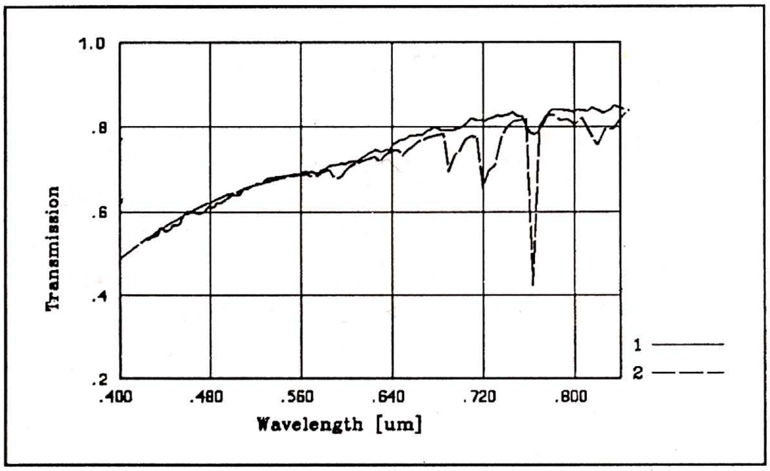

Fig. 3. Comparison between measured (1) and modelled (2) atmospheric transmission; measurement from Maracci, 1990.

The field boundaries of the study area were digitized within a GIS and the vectors transformed into digital raster maps. The results of this procedure are 5 digital maps of the main agricultural parameters with a spatial resolution of 10 m. As an example Fig. 2 shows the digital map of the landuse in the test-site.

Besides the extensive ground data collection selected fields were investigated more intensively. For 9 fields of different landuses, the biomass and water content was measured at three sample points in each field.

In coincidence with the overflight field spectroscopic measurements with the GER MARK IV Spectrometer of the DLR/Oberpfaffenhofen were conducted. The spectral reflectance of selected reference targets, like a sandy soccer field, irrigated lawn and bare soil was measured in the wavelength interval between 0.4 and 2.5 µm with a spectral resolution ranging from 2 nm in the visible to 6 nm in the NIR. These measurements enable the com-

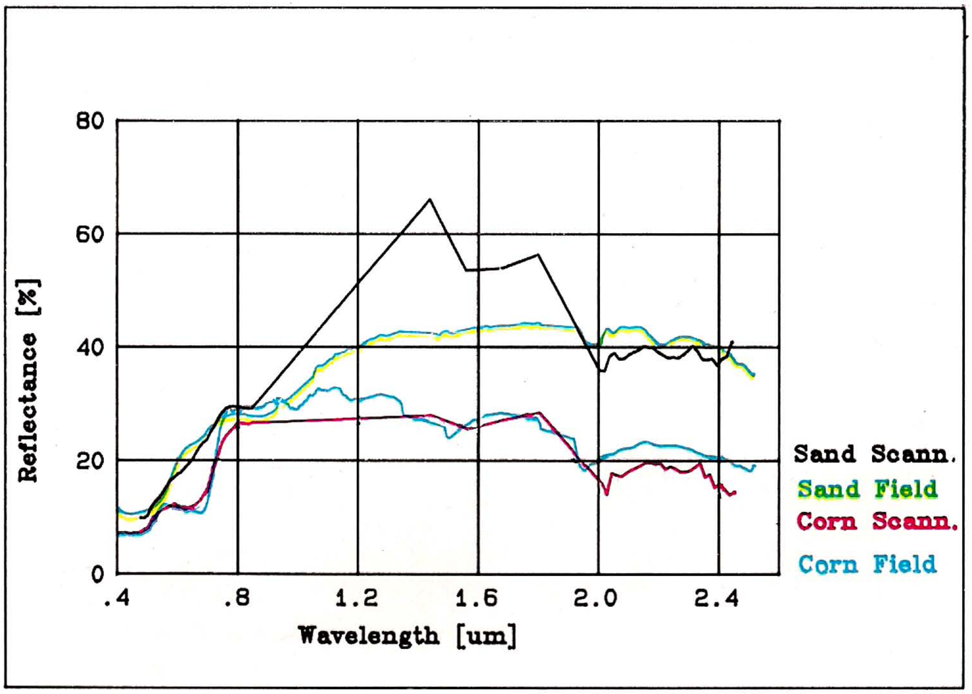

Fig. 4. Comparison between airborne and field spectra after conversion to reflectance values.

parison between field spectroscopic and airborne measurements.

4. RADIOMETRIC CALIBRATION

The GER-data was radiometrically corrected using the ground-measured reflectance spectra and atmospheric profiles from the German Weather Service as an input for the LOWTRAN-7 atmospheric model (Kneizys *et al.* 1988). LOWTRAN-7 includes the effects of multiple scattering, which have shown to be considerable in the short-wave region of the spectrum. First the path of the direct and diffuse radiance through the atmosphere to the ground was modelled. Then the radiance reaching the sensor was modelled by calculating the radiance that was reflected at the observed pixel in the direction to the sensor. This calculation takes into account the adjacent diffuse radiation and the path radiance. Modelling was carried out for all bands using the actual state of the atmosphere. Comparison between modelled atmospheric transmission and the actual atmospheric transmission, that was measured by Maracci during the over-flight (Maracci, 1990), show good coincidence, as can be seen in Fig. 3. The figure shows radiances.

The comparison between modelled and measured radiance at the sensor results in some modification of the GER-specifications. There is a wavelength shift of 12 nm towards the shorter wavelength in the first spectrometer, that could be determined through the reflectance maximum of vegetation in the green wavelength interval. Since the O_2- absorption at 760 nm can not be clearly identified in the scanner data, LOWTRAN-runs were carried out with different band-widths to simulate the GER-spectra. These calculations clearly indicate, that an assumed spectral resolution of 50 nm best fits the measured GER-spectra. This poor resolution may have its reason in a defocused spectrometer.

The GER-radiance data was transformed into reflectance data by first subtracting the path radiance from the measured radiance at the sensor (offset) and then applying a gain value derived from the model calculations. Fig. 4 shows resulting reflectance spectra of the GER-scanner in comparison with ground reflectance measurements of two different fields. To reduce noise the airborne spectra were averaged over the whole field. The difference between ground- and airborne spectra is largest in the 4 channels between 1.4 and 1.8 µm. It is almost impossible to calibrate these channels due to atmospheric effects.

Sensor dependent off-nadir-effects were eliminated using a statistical approach. The calculation of the column-statistics (mean, standard-deviation) over a large portion of the image (1000 rows) and a subsequent

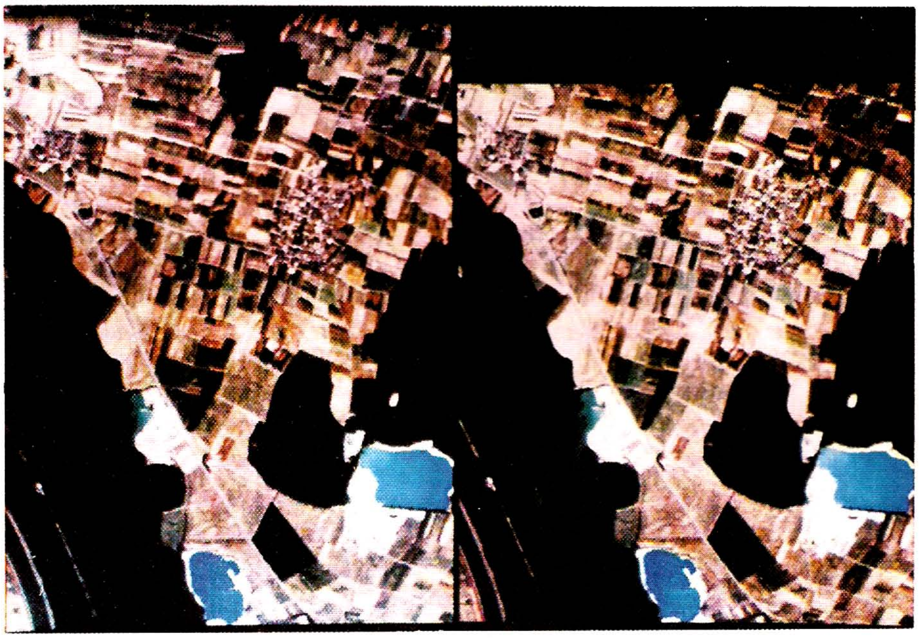

Fig. 5. Comparison between true color GER-data before (left) and after (right) radiometric homogenisation, bands:1, 7, 18.

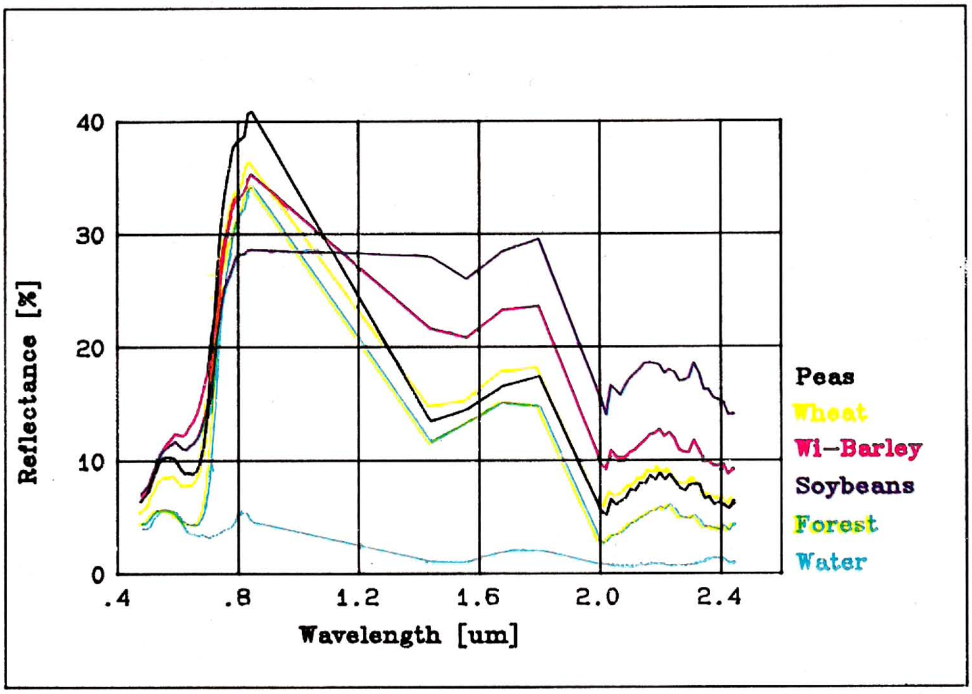

Fig. 6. Mean GER-spectra of different landuses.

fitting of a 2nd-order polynomial to the mean-values led to one correction-factor for each column and band. Fig. 5 shows the test-area in the visible part of the spectrum (left side = raw data; right side = look-angle corrected data). The brightening at large scan-angles can clearly be seen in the uncorrected data in Fig. 5 on the top and bottom (flight direction from left to right).

5. GEOMETRIC REGISTRATION

The GER-Scanner data were geometrically corrected to enable the combination between digital ground truth maps of measured plant parameters and the imaging spectroscopy data. For the geometric correction two steps were conducted:

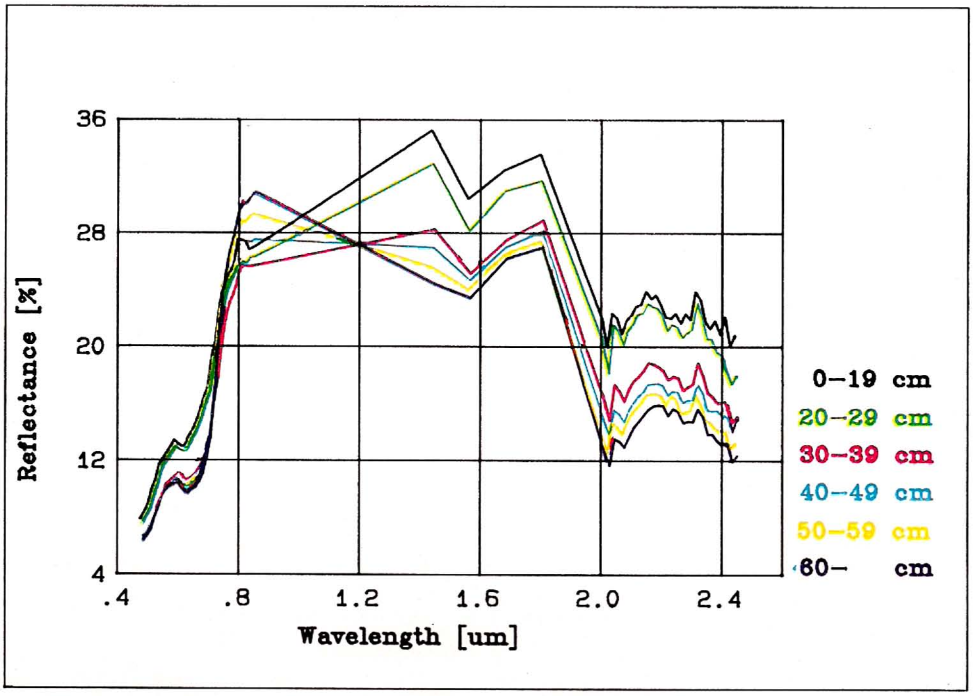

Fig. 7. Mean GER-spectra of corn with different plant height.

1) System-corrections: The delivered roll-corrected GER-scanner data were panorama corrected to remove the geometric scan effects. The undersampling of the airborne data was corrected and the resolution of the data was changed to be 10m, the same resolution as the digital ground data maps. For all geometric corrections the nearest neighbour method was used with the aim not to change the grey values themselves.

2) The remaining geometric distortions, that were caused by small aircraft movements, were corrected using 53 ground control pointes and a 2^{nd}-order polynominal.

These procedures lead to a mean deviation between scanner data and map of less then 1 pixel (app. 9m). Fig. 1 shows the GER-image after the geometric registration.

6. EVALUATION

The preprocessed scanner-data can be combined with the digital ground truth maps. This combination enables to analyse the information content of the scanner data in relation to the mapped plant parameters. One result of such an analysis is shown in Fig. 6. The digital map of the landuse (Fig. 2) was used in combination with the imaging spectroscopy data to separately average the spectra of all pixels in the test-area for each landuse. Peas (averaged spectrum of 2351 pixels) show the highest reflectance in the NIR. Winter-barley (4555 pixels) varies from wheat (app.1100 pixels) because winter-barley was already mature and there is no distinct chlorophyll absorption at 680 nm. Soybeans (8104 pixels) show a high reflectance in the MIR, that is due to the low soil cover of soybeans at the actual phenological stage and the high reflectance of the underlying soil. Forest (55460 pixels) is very dark especially in the visible, but can be easily distinguished from waterbodies (8162 pixels) in the MIR. The relative reflectance maximum of water at 0.8 µm can be explained through the high intensity of diffuse radiation, reflected from the vegetation surrounding the waterbodies (adjacency effect).

Another example of a combination between ground truth map and scanner data is shown in Fig. 7. For the whole test-site the pixels of corn were extracted and grouped in 6 classes of different plant height. For these classes the mean spectra were calculated. The spectra in Fig. 7 show obvious changes of reflectances with varying vegetation height. The differences are largest in the MIR and may be caused by decreasing influence of the soil signal on the signal of the pixel with increasing vegetation height

The changes to the spectral properties of the surface with irrigation can be investigated on one selected field, which

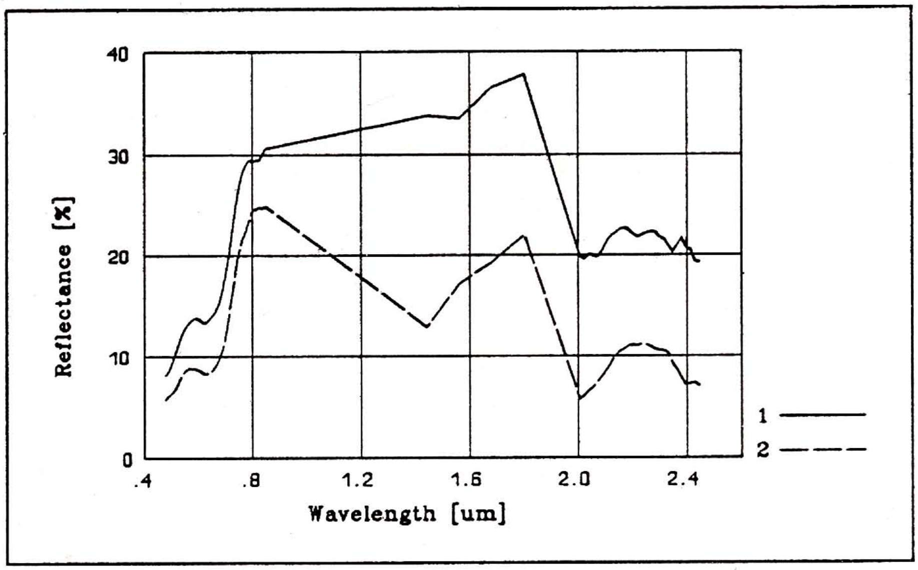

Fig. 8. GER-spectra of a partly non-irrigated (1) and irrigated (2) field of soybeans.

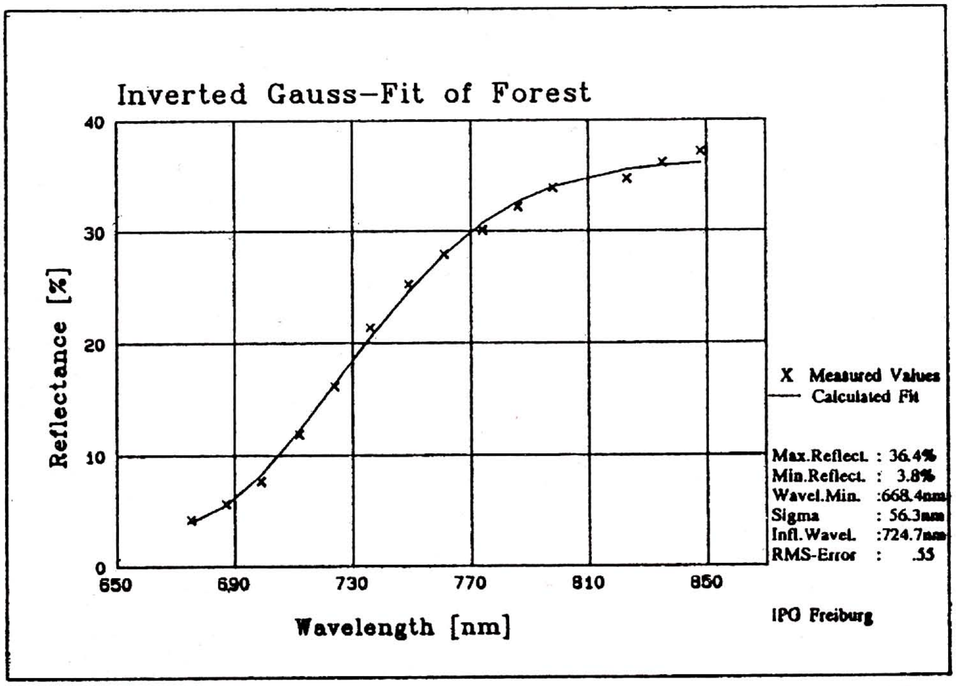

Fig. 9. Inverted Gauss-Fit of a GER-spectrum of forest.

was covered to about 20% with soybeans. This field was partly irrigated during the overflight. Fig. 8 shows the GER-spectra of two windows, which were put over the irrigated and non-irrigated part of this field. In the visible to NIR part of the spectrum the change in reflactance is quite moderate and the features of the spectrum are stable. There is mainly a reduction on reflectance by app. 25%. The change of the course of the reflectance in the MIR is much more distinct. The reflectance of the non-irrigated soybeans shows absorption structures of the underlying soil. On the irrigated part of the field these structures are hidden by the strong absorption (especially near 2.0 and 2.5 μm) of the water applied. The water absorption therefore not only causes a quantitative change in the reflectance but also a quantitative change in the course of the spectra in the MIR.

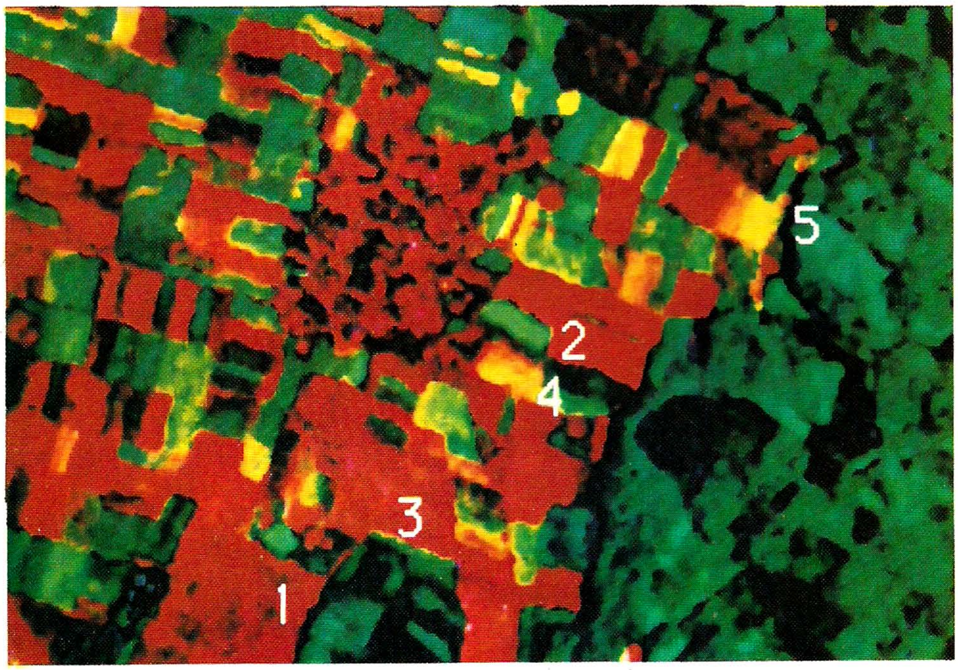

Fig. 10. Red-Edge image.

An attempt to compress the imaging spectrometer data was made by parametrizing the course of the reflectance in the wavelength interval from 670 to 850 nm with an Inverted-Gaussian Model (Bonham *et al.* 1988). An example of the result of this procedure for an airborne spectrum of forest is shown in Fig. 9. The inverted Gauss-model was applied to all pixels in the test-area. The resulting image was filtered using a 3x3 median filter to remove noise. This final 'red edge' image consists of 4 bands (minimum and maximum reflectance, wavelength minimum and sigma of the Gauss-function, which represent the course of the reflectance values of 14 bands in the NIR, which were used for the fit. As a great advantage of the procedure a root-mean error can be computed for the goodness of fit. For the whole image this deviation between the fitted and measured reflectances is 0.78%.

Three of the 4 parameters of the Gauss-fit (minim. and maxim. reflectance, inflection wavelength = wavelength minimum + sigma) are shown in Fig. 10 for a subarea of the test-site. In this representation bare fields show up in red (1 = 10% covered corn field) and vegetated areas show up in green (2 = peas). Since the vegetation in the test area experienced considerable water stress during the time of the overflight, the differences within single fields (3,4,5 = barley, oats with 100% ground cover) also represent changes in vegetation reflectance properties with plant water status.

7. CONCLUSIONS

The first analysis of the GER-Imaging- Spectroscopy data, that was gathered in the Freiburg test-area during the EISAC-89 campaign shows clearly, that the complexity of the spectral data strongly increases with the number of bands used. For the first time spectral features of the soils and the plants become visible in greater detail. To be able to compare the areal measurements with field-spectroscopy a careful removal of unwanted information, like atmospheric effects (absorption, scattering, angle) and scanner- effects (band-width, wavelength shift) has to be carried out. For this purpose tools have been developed and have to be further enhanced, that go beyond the methods of classical digital image analysis.

Working with Imaging-Spectroscopy data shows that ground-truth has to be taken with much more accuracy than when using low-spectral- resolution data, to be able to explain the measured effects. It is helpful to integrate the ground-truth in a GIS to have a spatial representation of the collected information together with the airborne data.

The first analysis of the preprocessed imaging spectroscopy data also shows that there is considerable information contained in the images on plant parameters like plant-height, soil-cover and irrigation. These parameters are of particular importance for the modelling of hydrologic processes like evapotranspiration. The models applied for this task rely much more on this kind of quantitative parameters than on the bulk- parameter land-use. For the plant parameters the information content in the MIR is especially interesting. To extract these important informations from the large amount of data available, data-reduction and data- extraction strategies have to be developed. These strategies will decide on the practical applicability of Imaging-Spectroscopy data.

Future instruments with better signal-to- noise ratios and enhanced spectral resolution will enable to work with the data on a pixel basis and will allow to differentiate between different parts of fields, where the same plant-species grows. If these instruments should be used for plant-studies they have to be equipped with channels in the MIR to take advantage of the large information content on soils and plants in this region of the spectrum.

ACKNOWLEDGMENT

The authors wish to thank JRC and ESA for financing and conducting the EISAC'89 campaign, the German Research Foundation (DFG) for funding the evaluations under the contract Ma 875/2-1, F. Lehmann for the use of the field-spectrometer and M. Maracci for the transmission data.

REFERENCES

Bonham - Carter, G.F., 1988, "Numerical procedures and computer program for fitting an inverted Gaussian model to vegetation reflectance data", in: *Computers & Geosciences*, Vol 14, No 3, pp.339-356.

Kneizys, F.X., Anderson G.P., Shettle, E.P., Gallery, W.O., Abreu, L.W., Selby, J.E.A., Chetwynd, J.H., Clough, S.A., 1988, "Users Guide to LOWTRAN-7", in: Environmental Research Papers No.: 1010; AFGL-TR-88-0177; Air Force Geophysics Laboratory.

Maracci, M., 1989, Personal communications, JRC-Ispra.

Mauser, W., 1989, "FAP - ein interaktives Programm zur Bearbeitung von Flächendaten; Version 1.0 - Benutzerhandbuch", Institut für Physische Geographie der Univeristät Freiburg, 300 Seiten, 1988.

Richter, R., 1990, Personal communications, DLR-Oberpfaffenhofen - Institut für Optoelektronik - Abteilung Spektrometrie und Modelle.